The *Cryptococcus* extracellular vesicle transcriptome

Adam TAHERALY[1], Corinne MAUFRAIS[1,2], Frédérique MOYRAND[1], Jessie COLIN[1,3], Jean-Yves COPPEE[1] and Guilhem JANBON[1]*

1. Institut Pasteur, Université Paris Cité, Unité Biologie des ARN des Pathogènes Fongiques, Département de Mycologie, F-75015, Paris, France

2. Institut Pasteur, Université Paris Cité, HUB Bioinformatique et Biostatistique, C3BI, USR 3756 IP CNRS, F-75015, Paris, France

3. Ecole Pratique des Hautes Etudes, PSL Research University, F-75014, Paris, France

* To whom correspondence should be addressed. Email: janbon@pasteur.fr

Abstract

Extracellular vesicles (EVs) are now recognized as key players in the biology of numerous organisms, including pathogenic fungi. However, studying EVs in these organisms remains challenging. The recent implementation of new protocols to purify EVs in the pathogenic yeast *Cryptococcus neoformans* has resulted in a more detailed description of their structure and protein composition. Although a few publications describing RNA molecules associated with EVs have already been published, we reasoned that these new protocols would be beneficial for gaining a deeper understanding of the EV transcriptome. We thus purified EVs and confirmed that some RNAs were associated with these EV extracts. Iodixanol gradient analyses also revealed that these RNAs co-sedimented with EVs. We then sequenced these RNAs in parallel with RNAs extracted from the very cells producing these EVs using different types of sequencing libraries. Our data confirm the presence of siRNAs and tRFs associated with EVs, some of which are enriched. We also identified some snoRNAs, which in *Cryptococcu*s are mostly borne by coding gene or lncRNA introns.

Extracellular vesicles (EVs) are membrane bounded particles released by cells into the extracellular space. EVs have been described in all organisms in which they have been looked for (Van Niel *et al.* 2018). In mammals, in which they have been extensively studied, they have been shown to participate in cell-to-cell communication during development and normal physiology (Van Niel *et al.* 2018). They can also play a positive or negative role in pathological situations such as cancer, diabetes, etc. (Van Niel *et al.* 2022). In most cases, RNAs (mRNAs, tRNA halves, miRNAs, siRNAs…) have been identified as the active 'message-bearing' molecules within EVs (Valadi *et al.* 2007). EV RNAs have also been shown to play major roles in host-pathogen interactions (Munhoz Da Rocha *et al.* 2020). Seminal examples in parasitic worms, pathogenic bacteria and plant and insect fungal pathogens have been published in recent years, revealing a widespread usage of this type of interaction during infections (Buck *et al.* 2014; Cui *et al.* 2019; Rutter *et al.* 2022; Sahr *et al.* 2022). Here also, some RNA molecules have been shown to be implicated in these interactions (Weiberg *et al.* 2013; Buck *et al.* 2014; Cui *et al.* 2019; Sahr *et al.* 2022).

EVs have been identified in fungi for the first time in 2007 (Rodrigues *et al.* 2007), and since then they have isolated from every class of fungi (Rizzo *et al.* 2020). In human pathogens, EVs have been shown to play a role in cell intercommunication impacting fungal drug resistance in biofilm or filamentation as well as fungal replication within macrophages and virulence (Bielska *et al.* 2018; Zarnowski *et al.* 2021; Bitencourt *et al.* 2022a; Honorato *et al.* 2022). Yet, the physical bases of the exchanged messages and their mechanism of action remain mostly unknown. By analogy with other systems, one can anticipate that some RNAs could play essential roles. In agreement with this hypothesis, long-distance action of EVs on *Cryptococcus* intracellular replication within macrophages can be abolished by EV RNase treatment (Bielska *et al.* 2018).

Cryptococcus neoformans is a pathogenic yeast responsible for 200 000 deaths every year in the world (Rajasingham *et al.* 2017) which has been listed as one of four human fungal pathogens of the "critical group" by the WHO (Fisher and Denning 2023). The production of polysaccharidic capsule, the synthesis of melanin, the production of diverse enzymes associated with its ability to grow at 37°C have been considered as the main *Cryptococcus* virulence factors (Kwon-Chung *et al.* 2014). More recently, EVs produced by pathogenic fungi have been suggested to be also key factors in fungal pathobiology (Rizzo *et al.* 2021a). Nevertheless, EVs studies in *Cryptococcus* have long been limited by cumbersome protocols needed to obtain sufficient EVs even though fungal EVs have been isolated for the first time in this species (Rodrigues *et al.* 2007). Indeed, the initial published protocols used extended cultures (2 to 3 days) in complete liquid medium and often required several liters of culture to obtain enough vesicular extract for a single experiment (Rodrigues *et al.* 2007). This extended duration for cultures also led some to believe that the obtained vesicles actually originated from dead cells with no physiological role (Brown *et al.* 2015). A new protocol published in 2019 by Reis and colleagues in which cells are grown on solid medium for 24h helped resolve this issue and partially address these criticisms (Reis *et al.* 2019). We recently used EVs isolated with this protocol to study the structure of *Cryptococcus* EVs using proteomics, nano flow cytometry, CryoEM/TM and genetic analyses (Rizzo *et al.* 2021b). These experiments revealed a spectacular diversity in size, shape and structure of *Cryptococcus* EVs and helped us to propose a structural model of *Cryptococcus* EVs in which these extracellular organelles are surrounded by capsular polysaccharide and decorated by GPI-anchored and membrane proteins (Rizzo *et al.* 2021b).

While these analyses have greatly improved our understanding of the structure and protein content of EVs produced by *Cryptococcus*, the other molecules associated with these vesicles, particularly their RNAs, remain superficially described (Rizzo *et al.* 2020; Rizzo *et al.*

2021a). In fact, despite a few published studies (Bitencourt *et al.* 2022b), there is no real consensus on the structure of the fungal EVs transcriptome. This is partly due to the lack of consensus on the protocols to be used to prepare vesicular extracts, but also to the diversity of sequencing and sequence analysis strategies used. For instance, there are three publications describing the results of RNA sequencing from *Cryptococcus* EVs (Peres Da Silva *et al.* 2015; Peres Da Silva *et al.* 2018; Liu *et al.* 2020). Even though these results clearly open up possibilities by describing RNAs associated with fungal EVs, neither the EV purification processes, nor the bioinformatics analyses have been standardized. Moreover, no enrichment analysis has been performed and further experimental validation is often missing. Therefore, it is difficult to estimate the share of simple contaminants within the pool of RNA species identified. Thus, although RNAs associated with fungal EVs have been reported in many species (Bitencourt *et al.* 2022b), the fungal EV transcriptome remains poorly described.

In the present study, we used the Reis protocol to purify EVs from three species of *Cryptococcus* and we studied their transcriptome. Furthermore, we implemented an additional purification step based on iodixanol density gradient to show that RNA molecules co-sediment with EVs. Finally, we used several types of RNA sequencing libraries and bioinformatic strategies to compare the cellular and vesicular transcriptomes in *C. neoformans*.

Material and Methods

Strains: The strains used in this study were *C. neoformans* KN99α (Nielsen *et al.* 2003), *C. deneoformans* JEC21 (Loftus *et al.* 2005) and *C. deuterogattii* R265 (Ma *et al.* 2009).

EV sample preparation. EV extracts were obtained as previously described (Rizzo *et al.* 2021b). Briefly, *Cryptococcus* cells were grown for 16-hour in liquid YPD at 30°C and plated onto 24 minimal SD agar medium dishes. The plates were then incubated at 30°C for 24 hours and scratched to collect the cells, which were then gently resuspended in cold 0.01 M PBS (filtered at 0.02 µm). To separate the supernatant from the cells, two successive centrifugation steps were performed at 5,000 *g* and 15,000 *g* for 15 minutes at 4°C. The resulting cell pellets were snap frozen ethanol/dry ice and stored at -80°C. EVs were then pulled down from the 0.45 µm filtered supernatant by ultracentrifugation at 100,000 *g* for 1 hour at 4°C using a SW 40Ti rotor. The resulting pellet was resuspended in 400 µL of filtered 0.01 M PBS. When necessary, EVs were further purified on 40-5% w/v iodixanol gradient as previously described (Reis *et al.* 2021). After 18 h of ultracentrifugation at 100,000 *g* 4°C, fractions of 1 mL were collected by pipetting to which 9 mL of filtered 0.01 M PBS were added prior ultracentrifugation (1h 100,000 *g* at 4°C). Each pellet was then resuspended in 100 µL of filtered 0.01 M PBS and stored at 80°C.

RNA extraction: Both EV and cellular RNA extractions were carried out using a TRIzol protocol under RNAse-free conditions at 4°C as previously described (Moyrand *et al.* 2008).

UREA-PAGE : Heat denatured RNA samples were run in TBE-UREA 8M gel for 70 minutes at 120V. The gel was then washed with water and revealed using SYBRGold (Invitrogen) as suggested by the manufacturer.

RNA sequencing:

For the first strategy, total RNA was treated with Cap-Clip Acid Pyrophosphatase (Cellscript). as previously described (Wallace *et al.* 2020). The sequencing libraries were then constructed using the QIAseq® miRNA Library Kit according to the manufacturer protocol. The

sequencing reaction per se were performed using Illumina Iseq100. For small RNA libraries, 20-30 nt RNA molecules were UREA-PAGE purified from both EV and cell samples. RNA was precipitated using a DNA Lo Bind tube (Eppendorf) and recovered in 16.5 µL of water. Triphosphate in 5' were removed using a RNA 5' polyphosphatase (Euromedex Lucigen) and RNA were purified using 3 volume of absolute isopropanol and 1.8 volume of Agencourt RNAClean XP beads (Beckman). RNA was eluted with 6 µL of water. After ligation of an adaptater (5'rApp/NNNNTGGAATTCTCGGGTGCCAAGG/3ddC/) in 3', RNA was purified again. An adaptater (5'GUUCAGAGUUCUACAGUCCGACGAUCNNNN3') in 5' was added, and RNA was purified as described previously. RT reactions were performed using 5X SuperScript III (Invitrogen) using conditions suggested by the manufacturer. Libraries were finally amplified using Phusion PCR (10 for cell samples and 14 for EVs samples), checked by TapeStation electrophoresis. UREA-PAGE purified cDNA was then sequenced by Illumina NextSeq 500. Finally, strand-specific, paired-end cDNA libraries were prepared from cell or EV total RNA by polyA selection using the TruSeq Stranded mRNA kit (Illumina) according to manufacturer's instructions. Then, 100 bases were sequenced from both ends using an Illumina HiSeq2500 instrument according to the manufacturer's instructions (Illumina). Trimmed reads were mapped to the *Cryptococcus* genome using Bowtie2 (Langmead and Salzberg 2012) and Tophat2 (Kim *et al.* 2013) as previously described (Wallace *et al.* 2020).

Bioinformatics analysis: Data preparation, analysis, and visualization were conducted using BASH and R 4.3, unless stated otherwise. For the conservation plot, genomic sequences were obtained from FungiDB, including 1000 nucleotides before the start codon and after the stop codon. Homologous sequences from *C. deneoformans* JEC21, *C. deuterogattii* R265, *Kwoniella mangroviensis* CBS 8507, *Kwoniella heveanensis* CBS 569, *Tremella mesenterica* DSM 1558, and *Kwoniella bestiolae* CBS 10118 were identified using blast and retrieved in the

same manner. Alignment was performed using MUSCLE 5.1 (Edgar 2004), and visualization was done using JalView 2.11.2.7. Conservation plot data were obtained using plotcon (EMBOSS 6.6) (Rice *et al.* 2000) with a window size of 20 nucleotides.

Proteomic analysis: Proteomic analysis was performed as described previously (Rizzo et al., 2021). However, in order to eliminate the iodixanol remaining in the gradient purified samples, proteins were first TCA precipitated before being resuspended in PBS and trypsin digested.

Results

Some RNAs are EV-associated in *Cryptococcus.*

Numerous studies have documented the presence of RNA molecules associated with fungal EVs, including in *Cryptococcus* (Peres Da Silva *et al.* 2015; Peres Da Silva *et al.* 2018; Liu *et al.* 2020; Reis *et al.* 2021; Bitencourt *et al.* 2022b). Nevertheless, the methods of growth, EV purification, and RNA sequencing employed in these studies vary significantly. We also know that the growth conditions can have a strong influence on EV production and EV composition in fungi (Reis *et al.* 2021; Amatuzzi *et al.* 2022; Rizzo *et al.* 2023). This suggested that further analyses would be beneficial for gaining a deeper understanding of the fungal EV transcriptome structure. We here isolated total RNAs from EVs purified from cells cultivated on solid minimum medium, following the established procedure (Reis *et al.* 2021; Rizzo *et al.* 2021b). We then loaded these isolated RNAs onto denaturing urea polyacrylamide gel (Urea-PAGE) alongside RNAs obtained from the cells generating these EVs (Figure 1A). As anticipated, SYBR Gold staining confirmed the presence of RNAs in both cell and EV extracts, indicating that certain RNA molecules are associated with EVs in *C. neoformans.* To further validate this association, we deposited the EV extract on an iodixanol density gradient (Ford *et al.* 1994) (Figure 1B). After 18h of ultracentrifugation at 100 000 *g*, we observed a single whitish ring at a centered position within the otherwise transparent gradient (Figure 1B). Examination of twelve gradient fractions using both flow cytometry with a NanoFCM^{TM} apparatus and ergosterol concentration evaluation (Rizzo *et al.* 2021b; Rizzo *et al.* 2023) showed that the majority of EVs are found within the fractions 6, 7 and 8 (Figure 1C). In fact, the 7th fraction, which corresponds to the whitish ring position, exhibited the highest concentration of EVs, strongly suggesting that this ring corresponds to concentrated EVs. We then conducted proteomic analysis on all twelve fractions. The assessment of protein relative abundance using Intensity Based Absolute Quantification (IBAQ) (Schwanhäusser *et al.* 2011) further corroborated this observed pattern (Figure 1D) (Table S1). The previously

described most abundant proteins in *C. neoformans* EVs, Mp88 and Vep1, represent here 58% of the total proteins confirming that these proteins are the major EV proteins in *C. neoformans* (Rizzo *et al.* 2021b). We then isolated RNAs from each of the 12 fractions and analyzed these extracts by Urea-PAGE. SYBR Gold staining unveiled that a significant portion of the RNA was linked to fractions 6, 7, and 8, which also contained EVs and EV proteins. Overall, these analyses provide further evidence that the RNAs purified from our initial EV extract are indeed associated with EVs, in line with previous reports (Bitencourt *et al.* 2022b). However, the precise localization of these RNAs, whether inside, on, or at the surface of the EVs, still requires further investigations.

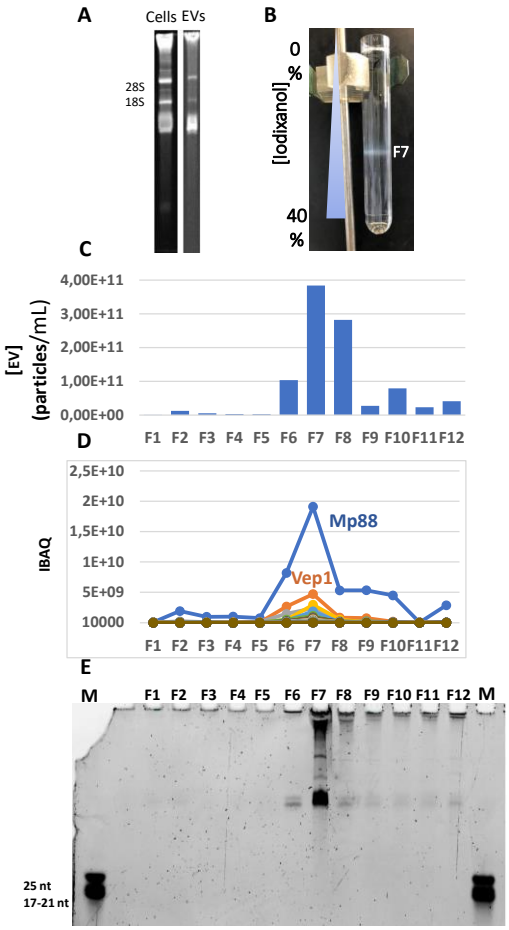

Figure 1. Some RNA molecules are EV associated. (A) Urea-PAGE analysis of cells and EV RNA extracts. (B) Picture of a tube of iodixanol gradient revealing a whitish ring containing EVs around the fraction 7. (C) EV concentration within each fraction evaluated by NanoFCM^{TM}. (D) Proteomic analysis of the iodixanol gradient fractions confirming the

prevalence of Mp88 and Vep1 in *C. neoformans* EVs. (E) Urea-PAGE analysis of RNAs purified from each fraction of the iodixanol gradient. EV concentrations evaluation and proteomic analyses were performed on the same gradient. RNAs were extracted from samples obtained from an independent experiment.

Small RNAs associated with EVs

Because a large diversity of RNAs (siRNAs, tRNA halves, lncRNAs, mRNAs, snRNAs, snoRNAs…) have been shown to be associated with EVs in different organisms including fungi (Rizzo *et al.* 2021a; Bitencourt *et al.* 2022b), we first constructed a sequencing library using a small RNA library preparation kit on total RNA extracted from EVs and previously submitted to decapping treatment (Wallace *et al.* 2020), yet no size selection step was implemented at this step. We reasoned that this approach should provide us with a comprehensive view of the *Cryptococcus* EV transcriptome since it should generate small RNA reads as well as, albeit to a lesser extent, longer reads up to 100 nt corresponding to mRNAs or lncRNAs fragments from the same samples. We mapped a total of 1.4 million of reads to the *C. neoformans* H99 reference genome (Janbon *et al.* 2014). A substantial portion of the reads longer than 17 nt (38%) aligned with the ribosomal DNA loci or the mitochondrial genome. The remaining reads exhibited a median size of 26 nt. Among them, the majority (98.3%) mapped to annotated nuclear genome features, either in the sense or antisense orientation. We noticed that most reads aligning in the sense orientation (81.7%) were short reads (median size = 27 nt) aligning to tRNA loci. However, it was obvious that the current annotation of tRNAs was partial with number of them not annotated and several others for which the genomic coordinates were wrong. We thus used tRNAscan (Chan *et al.* 2021) to re-annotate the tRNAs in the *C. neoformans* genome adding 8 pseudo-tRNA loci and updating the coordinates for three tRNAs (CNAG_10023, CNAG_10007, CNAG_10077) (Data S1). The analysis of our sequencing data then revealed that 72.8% of the sense reads

mapped to the 3' and 5' regions of the annotated tRNAs in *C. neoformans* (Figure 2A, C) suggesting the presence of tRFs (tRNA fragments) in the transcriptome of *C. neoformans* EVs. These tRFs have previously been identified as associated with EVs from different organisms (Lambertz *et al.* 2015; Chiou *et al.* 2018; Artuyants *et al.* 2020; Gámbaro *et al.* 2020). In mammals, tRFs hold promise as biomarkers and have been shown to play diverse regulatory roles in various cancers, neurodegenerative diseases, and responses to infections (Pandey *et al.* 2021). Some tRFs have been shown to associate with Argonaute protein (Ago) in different organisms and several studies reported the role of tRFs in the RNA interference pathway (Maute *et al.* 2013; Ren *et al.* 2019; Sharma *et al.* 2023). Reads aligned to tRNA sequences have already been detected in EV transcriptomes including in human fungal pathogens (Peres Da Silva *et al.* 2015; Munhoz Da Rocha *et al.* 2021). Yet, tRFs functions in these organisms remain to be identified (Jöchl *et al.* 2008). Similarly, although our analysis revealed that a subset of these tRNAs are overrepresented (Pro-tRNA (CGG and UGG), Leu-tRNA (AAG), Gly-tRNA (UCC), Gln-tRNA (CUG) and Asp-tRNA (GUC)) (Figure 2C), the mechanisms underlying this enrichment remain unknown. We performed the same experiment in *C. deneoformans* and *C. deuterogattii* and observed similar pattern at the tRNA loci.

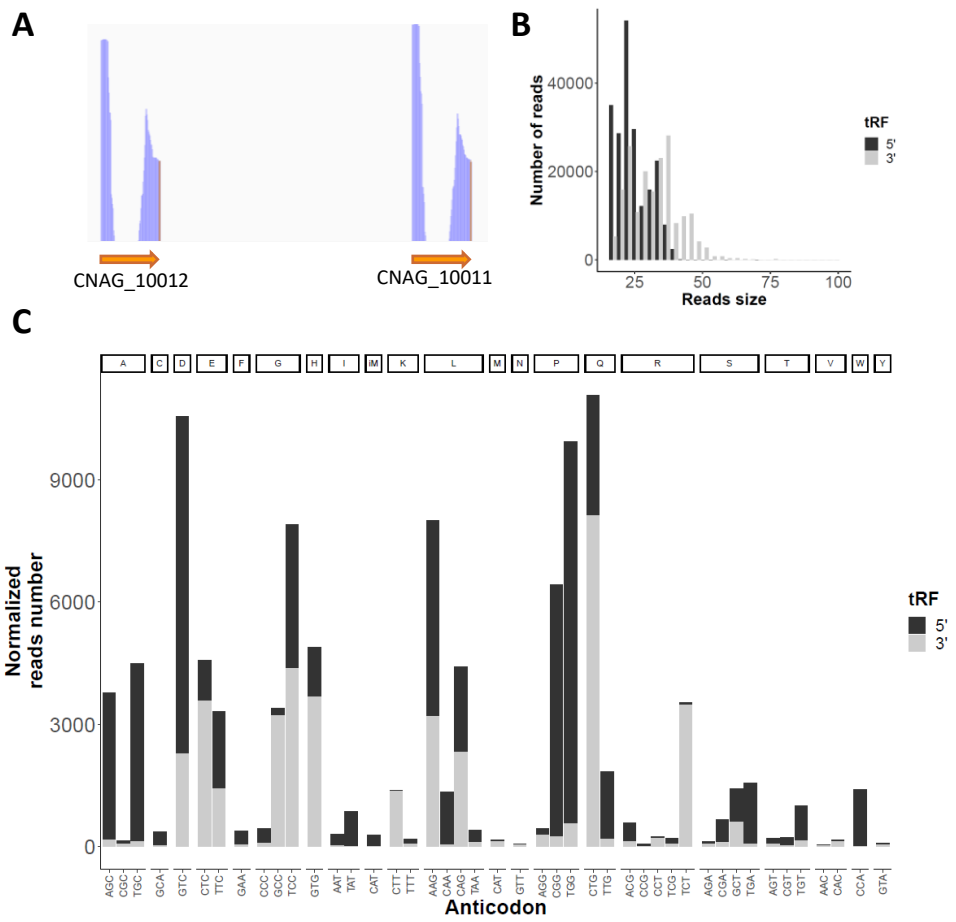

Figure 2. tRFs are associated with *Cryptococcus* EVs. (A) Example of RNA-seq pattern at tRNA loci as visualized by IGV at the loci CNAG_10012 and CNAG_10011 both encoding tRNAs. (B) Number and size of small reads aligned to tRNA loci. (C) RNA-seq reads number associated with the different tRNAs in *C. neoformans*.

By contrast, the examination of reads mapping in the antisense orientation to annotated features showed a significant enrichment of reads ranging from 20 to 25 nucleotides in length, all starting with a uridine. These features are typical of small interfering RNAs (siRNAs) (Figure 3 A, B) (Dumesic *et al.* 2013). As expected, these reads are antisense of transposons or transposon-like sequences (Janbon *et al.* 2010; Dumesic *et al.* 2013) (Table S2). Additionally, we observed a significant number of these siRNA-like reads mapping within the centromere of all chromosomes, which is consistent with the documented transposon-richness

of the centromere structure in *Cryptococcus* (Yadav *et al.* 2018). We performed the same experiment using EVs extracted from *C. deneoformans* and *C. deuterogattii*. The small RNA profile in *C. deneoformans* EVs was very similar to the one obtained in *C. neoformans*. By contrast, as expected, in the RNAi-deficient species *C. deuterogattii*, no siRNA-like species were detected in EVs transcriptome (not shown).

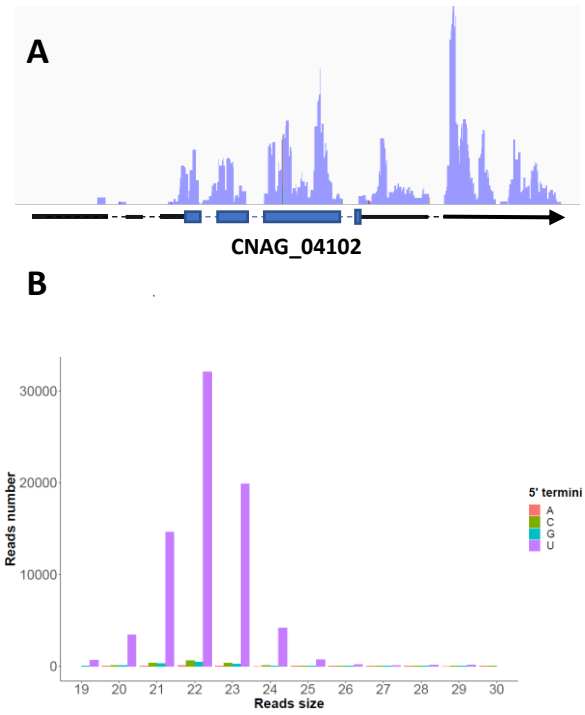

Figure 3. siRNAs are associated with EVs in *C. neoformans*. (A) IGV visualization of antisense reads alignment at the CNAG_04102 locus. (B) Bar plot graph depicting the number of antisense reads as a function of their size and the nature of the 5' terminal nucleotide.

To assess whether the EV small RNA transcriptome differs from that of the cells, we purified on gel 20-30 nt small RNAs from both EVs and cells producing EV to construct small RNA-seq libraries. This experiment was conducted in triplicate and 3.8 to 5.6 million reads obtained from EV libraries and 8 to 9.9 million reads from cell libraries were aligned to the *C. neoformans* genome. Again, most of the reads (98% and 98.6% in EVs and cells, respectively) were either tRFs or siRNAs although their proportion was not identical to the one obtained through sequencing RNAs without implementing a size selection step. By

counting reads aligning on arbitrarily defined 500 bp genomic regions, we identified 86 regions containing annotated features with abundant normalized read counts (>100 reads) enriched or depleted in the EV samples compared to the cell samples (Figure 3A) (Table S3). At eight of these loci, the coverage was due to GAU repeat microsatellite-like sequences that were enriched up to 514-fold in EVs. However, the presence of similar reads in the sequencing data, presenting the same repeats but in larger numbers, and which did not align to the genome might suggest that these reads could be artifacts. The most enriched region was specific for reads nearly exclusive of the EVs with an 897-fold enrichment. This 21-nt long read looks like a siRNAs (5' TTTCACCAACGCCGCTACCAG 3') and aligned in sense to the Rrp36 ribosomal protein encoding gene at the CNAG_03284 locus (Table S3). Moreover, 74 of these EV enriched regions correspond to tRFs (Table S3). Interestingly, at 36 tRNA loci, the ratio of 5' tRF vs 3' tRF reads numbers was statistically different between the cell and the EV samples. For instance, at the CNAG_10094 locus, the 5'tRF is 9.4-fold more abundant in EVs than in the cells whereas the amount of the 3'tRF reads is barely modified (0.8-fold) (Fig 3B). A similar pattern although reverse was observed at the CNAG_10061 locus. Overall, this analysis revealed the presence of siRNAs and tRFs associated with EVs in *Cryptococcus.* The specific enrichment of a subset of small RNAs in EVs suggests a specific mechanism of targeting. In agreement with this model the single Argonaute protein Ago1 was identified in the EV proteome (Table S1)

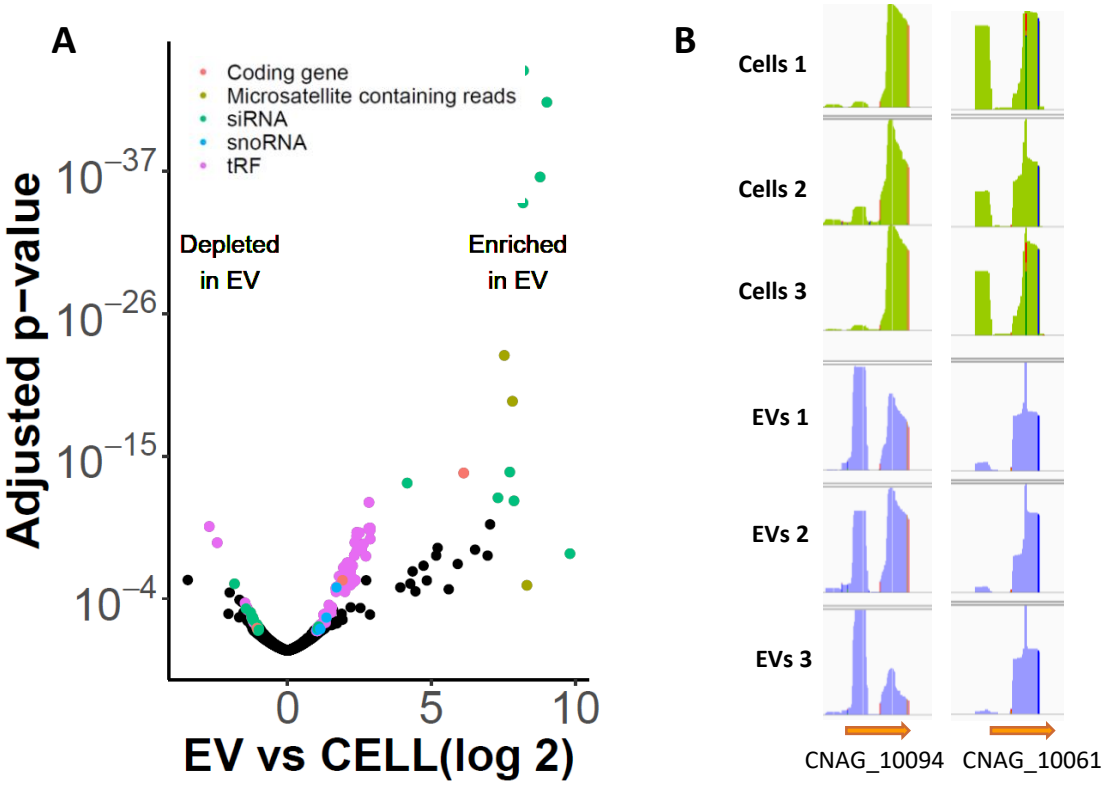

Figure 4. Bias in EV vs cell small RNA content. (A) Volcano plot illustrating the difference between the small RNA transcriptome in EVs and the cells producing these EVs (B) IGV visualization of examples of alteration of the 5'tRF vs 3'tRF repartition in EVs compared to cells at two tRNA loci. Three replicates of the experiment are shown.

SnoRNAs and other RNAs of intermediate size are associated with EVs

The analysis of the sequencing data obtained from total EV RNA samples also identified long reads (>70 nt) (2%, n = 11928) aligning to the *C. neoformans* genome. These reads aligned to 105 precise genomic regions. Most of them (n = 101) correspond to annotated regions, lncRNAs or coding genes, and, surprisingly, a large proportion of them (n = 61) were positioned within introns (Figure 5A). Although these regions did not resemble to any sequence with a known function available in the databases, iterative alignments using BLAST and structure analyses using the RFAM database (Kalvari *et al.* 2021) suggested that number of these sequences are snoRNAs. Further analyses of the sequences data identified 67 snoRNAs with C/D boxes, displaying a classical kink-turn (stem-bulge-stem) structure and characterized by two main terminal consensus sequences (*i.e.* the C box (RUGAUGA) and the

D box (CTGA)). Interestingly, even when only fungi closely related to *Cryptococcus* are considered, the sequence of these introns is not well conserved except for the central region containing the snoRNA. For the snoRNAs carried by lncRNAs, this situation is even more remarkable as the only part of the lncRNAs evolutionary conserved is the part bearing the snoRNAs. Actually, the poor exon sequence conservation in these lncRNAs suggests that their roles might be restricted to the production of these snoRNAs. A representative example of a lncRNA-bearing-snoRNA sequence conservation pattern in close *Cryptococcus* relative species is given on the figure 5B. Outside of these close relative species the sequence conservation of the snoRNA sequences is restricted to the consensus boxes.

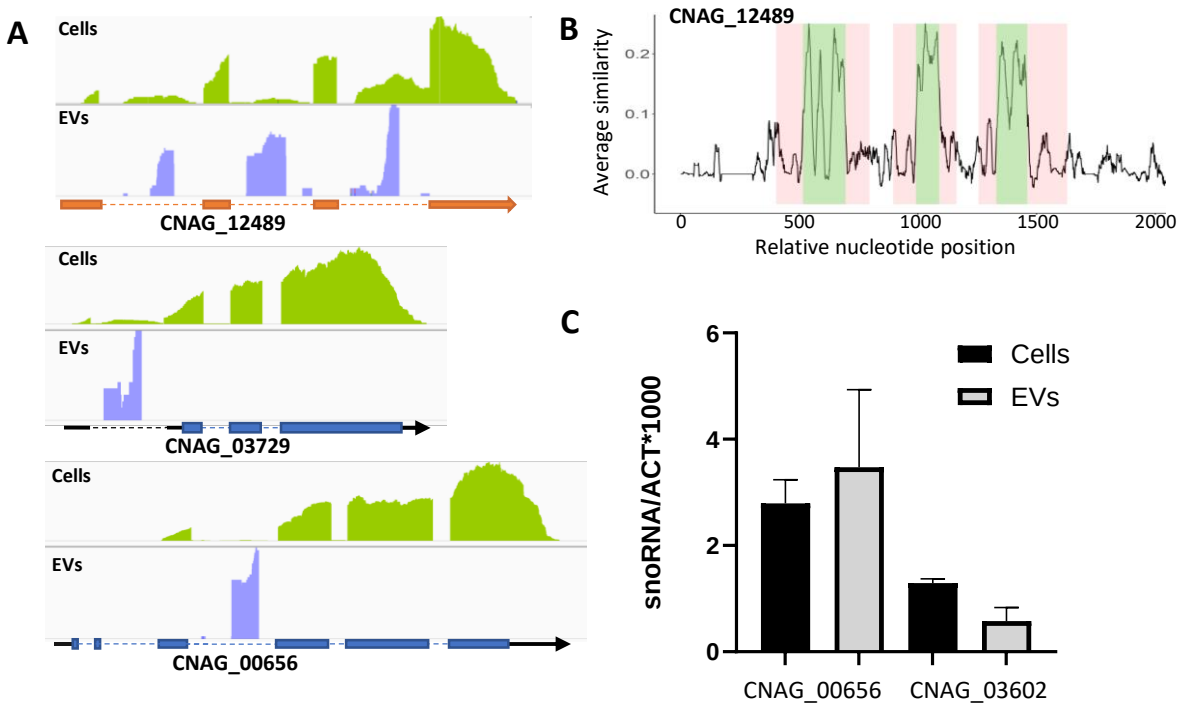

Figure 5. SnoRNAs are associated with EVs in *Cryptococcus*. (A) Examples of snoRNAs associated coverage as observed by IGV. The lncRNA CNAG_12489 encodes three intronic snoRNAs. The coding genes CNAG_03729 and CNAG_00656 contain a snoRNA in a 5'UTR and CDS intron, respectively. (B) Sequence alignment of close *C. neoformans* relative species (*C. deneoformans, C. deuterogattii, Kwoniella heveanensis, Kwoniella bestiolae and*

Kwoniella dejecticola) orthologous loci, revealed that the sequence conservation is restricted to the portion corresponding to the snoRNAs within the introns. The green regions correspond to the snoRNA sequences whereas the intronic sequence outside are highlighted in pink (C) snoRNAs do not seem enriched in EVs as revealed by RT-qPCR.. Experiments were conducted in triplicate on RNAs extracted from EVs or cells producing EVs.

We also identified 29 snoRNAs with H/ACA boxes. However, whereas 83.6% of snoRNAs with C/D boxes are in introns, most H/ACA boxes (55.2%, n =16) are located within lncRNAs and one in the intron of a lncRNA. Few of them were located in 5'UTR (n=2), 3'UTR (n=4) or introns (n=4) of coding genes. One snoRNA was overlapping the CDS and the 3'UTR of CNAG_03007 (*CPC1*) suggesting an annotation issue. The remaining snoRNA H/ACA was located within an intergenic region between the CNAG_06094 and the CNAG_06095 loci. We here annotated it as CNAG_13211. In these cases, the sequence conservation with other fungi outside of close relative is also restricted to the consensus boxes. Visual comparison on IGV of our dataset from EVs or EVs-producing cells (Rizzo *et al.* 2023) suggested that snoRNAs might be enriched in the EV RNA samples (Figure 5A). However, RT-qPCR experiments performed on total RNA purified from EVs and EVs-producing cells did not confirm this impression, highlighting the need of experimental confirmation in this type of analysis (Figure 5C). Analysis of the *C. deneoformans* and *C. deuterogattii* EV sequencing data revealed a similar profile and a very high conservation of these sequences in the three *Cryptococcus* species.

In the EV transcriptome, we also found reads associated with lncRNAs with no annotated function. We manually curated the corresponding annotation and performed RFAM analysis to identify their putative function (Data S1). We identified this way the five main spliceosome components. U1 (CNAG_12993), and U2 (CNAG_12573) were structurally well annotated but had no assigned function. U4 (CNAG_13128) annotation was changed to fit the reads

alignment profile. U6 (newly annotated locus CNAG_13208) located in the region between CNAG_05444 and CNAG_05445 was not annotated. U5 was present within the 5'UTR region of the coding gene CNAG_01093, but the alignment profile of the reads from both EVs and cells suggested that the transcription of U5 and CNAG_01093 might be independent. This is supported by the presence of a thymine stretch at the 3' end of the putative U5 locus, which is a characteristic of RNA polymerase III transcription termination. We thus reannotated this locus, CNAG_13209 being U5. We also identified the loci CNAG_12266 and CNAG_12660 as the RNA moiety of the RNases P and MRP, respectively. Finally, we annotated the 7SL ncRNA at new locus CNAG_13210.

PolyA RNAs in EVs

We also prepared RNA-seq libraries from polyA+ RNA of EV samples in triplicate. Because the first replicate yielded a very low number of reads, it was subsequently excluded from further analysis. Reads were then aligned to the *C. neoformans* H99 reference genome (Janbon *et al.* 2014) and the number of reads aligned to each annotated feature was counted (Wallace *et al.* 2020). We used this counting to compare the mRNA and lncRNA abundances in EVs and in cells producing these EVs (Rizzo *et al.* 2023). Our analysis did not reveal spectacular enrichment of any mRNA in EVs (Figure 6). Among the genes with at least 100 reads in both EV and cell samples, the most enriched mRNA (5.06-fold) in EVs (CNAG_07756) encodes a *C. neoformans* ubiquitin-protein transferase activating protein Cdc20 homolog. It is important to note that this analysis was limited by the fact that number of genes and lncRNAs have no read in at least one EV or cell replicate. Overall, as no outliers were identified, it is difficult to draw definitive conclusions regarding specific mRNA or lncRNA enrichment in EVs.

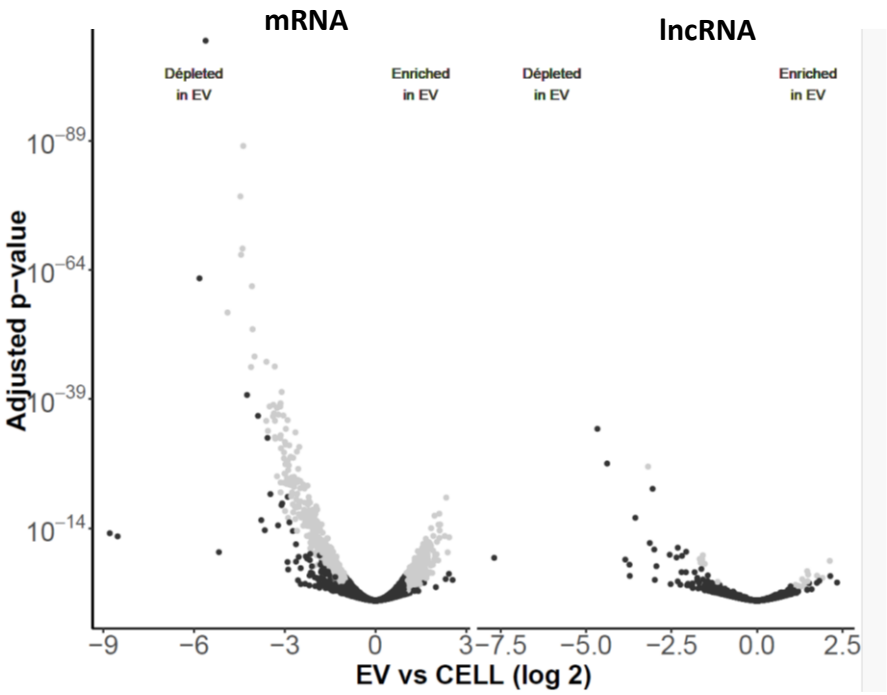

Figure 6. Volcano plot illustrating the difference between the polyA+ RNA transcriptome in EVs and in the cells producing these EVs

Discussion

We and others have produced a large quantity of data describing the structure and the dynamics of the *Cryptococcus* cellular transcriptome (Janbon *et al.* 2014; Gonzalez-Hilarion *et al.* 2016; Gröhs Ferrareze *et al.* 2021; Kalem and Panepinto 2022). However, even though the study of extracellular transcriptome has become a hot topic in number of organisms including microbes (Hulstaert *et al.* 2020; Pita *et al.* 2020; Gruner and Mcmanus 2021), the diversity of RNA molecules secreted by these yeasts remain poorly described. In fungi, the extracellular transcriptome has been mostly studied through the analysis of RNA molecules associated with EVs (Bitencourt *et al.* 2022b). Several papers reported the presence of small RNAs as well as polyA+ RNAs associated with fungal EV extracts (Bitencourt *et al.* 2022b). However, due to the heterogeneity of the protocols used to prepare these extracts, the diversity of strategies employed for sequencing library preparation and data analysis, as well as the general absence of experimental validation, the overall picture remains blurry. We here used a standardized and validated protocol to prepare EV extracts from three *Cryptococcus* species, we demonstrated that EVs and RNAs co-sediment in an iodixanol based density gradient. We purified and sequenced these RNAs in parallel with RNAs extracted from the very cells producing these EVs. We finally analyzed this data using a structurally and functionally improved genome annotation. None of the data we have produced is entirely new and they mostly strengthened and improved previous results obtained by other teams. As previously reported (Peres Da Silva *et al.* 2015), we identified a large number of tRF reads in the vesicles transcriptome but we here used an improved version of the tRNA annotation in *C. neoformans* to better quantify them. Our analysis also reveals for the first time that at certain tRNA loci, the proportion of 5'tRF vs 3'tRF is altered in EVs compared to cells suggesting specific targeting mechanisms. The origin of the tRFs in *Cryptococcus* is still

unknown as no angiogenin (Kumar *et al.* 2016) homolog can be identified in these species. Interestingly, the siRNA deficient strain has conserved a Dicer homolog encoding gene in his genome (D'souza *et al.* 2011) but its role in the biogenesis of the tRFs remains to be studied. Similarly, the presence of reads specific of snoRNAs in fungal EV-associated small RNAs sequencing data was already reported (Peres Da Silva *et al.* 2015). We here extended this information by omitting the size selection step in a small RNA library sequencing kit protocol. Our results allow us to complete the characterization of the *Cryptococus* snoRNAome (Canzler *et al.* 2018; Kalem and Panepinto 2022). Yet, we did not observe a specific enrichment in EV extract for the two snoRNAs we checked by RT-qPCR. It does not mean that these are contaminants and that they have no function in EVs. For instance, the argonaute protein WAGO which has been reported to play a major role in EV biology in the parasitic worm *Heligmosomoides bakeri* is not particularly enriched in EVs compared to the cell (Chow *et al.* 2019). Similar data has been published in mammals in which EV-mediated communication is supposed to rely mostly on miRNA exchange (Weaver and Patton 2020). Besides, the H/CA ribonucleoprotein complex subunit 3, Nop10 (CNAG_01049) was found in our EV proteomic analysis (Rizzo et al 2023) which is in agreement with an active targeting of some snoRNAs to EVs. Our research also confirmed the very poor conservation of snoRNA sequences in fungi. It also suggested that some lncRNA unique function may be to encode snoRNAs in their intron. Finally, we confirmed the presence of siRNAs associated with *C. neoformans* EVs which has been previously reported in both *C. neoformans* and *C. deneoformans* (Peres Da Silva *et al.* 2015; Liu *et al.* 2020). Their structure and the fact that we cannot identify them in the RNAi-deficient species *C. deuterogattii* strongly suggested that these are genuine siRNAs (D'souza *et al.* 2011). As expected, and in agreement with the *Cryptococcus* literature, siRNA reads aligned to transposons or transposon-like sequences (Janbon *et al.* 2010; Dumesic *et al.* 2013). Here also, the analysis of the proteome data

revealed that the unique *C. neoformans* Argonaute protein is associated with EVs suggesting an active targeting of siRNAs. The presence of siRNAs associated with EVs is not unique to *C. neoformans* (Peres Da Silva *et al.* 2015) and seems to be a general pattern in fungi. In the recent literature, some of these siRNAs have been identified as miRNAs (Peres Da Silva *et al.* 2015; Liu *et al.* 2020). However, identifying miRNAs in a fungal species by aligning sequences to mammalian miRNAs remains a questionable strategy. In fact, the re-analysis of miRNAs and miRNA-like molecules identified in fungi has demonstrated that none of these newly miRNAs identified passed the various quality criteria (Johnson *et al.* 2022). At this stage, a miRNA-like role of some of these siRNAs cannot be ruled out without experimental confirmation.

The functions of these EV-associated RNA molecules remain unknown, but the literature is full of examples of cell-to-cell communication mechanisms based on RNA molecules exchanges within the same species but also between species including in host-pathogen interactions (Tsatsaronis *et al.* 2018; Cai *et al.* 2021). Although *C. neoformans* EVs have been deeply studied for their structure and composition, their very role in the communication between cells but also during the interaction with the host remain to be uncovered. Examples of EV-mediated exchanges of RNA species (such as siRNAs, miRNAs, tRFs or snoRNAs) between cells are flourishing both in pathogenic and non-pathogenic settings (Weiberg *et al.* 2013; Buck *et al.* 2014; Rimer *et al.* 2018; Ren *et al.* 2019; Sahr *et al.* 2022). These results suggest that this type of exchanges might exist as well in *Cryptococcus* although the characterization of the associated mechanisms remain very challenging.

Acknowledgements

We here want to thank Eugene Gladyshev and Sebastian Castro Ramirez (Institut Pasteur) for their help in the construction of small RNA libraires. We want Mariette Matondo and Thibault Chase from the Institut Pasteur proteomic facilities for proteomic data production and analysis. The work on EVs in the Janbon's laboratory is supported by the ANR grants ResistEV (AAPG2021 CE35) and FEVCOM (AAPG2023 CE35). A.T. is funded by a PhD Fellowship from Ecole Doctorale BioSPC, Université de Paris, 75006 Paris, France.

Table S1: Proteomic analysis of iodixanol gradient fractions

Table S2: Genes targeted by EV-siRNAs in *C. neoformans*

Table S3: list of the loci enriched in EVs vs cells in small RNA-seq data.

References

Amatuzzi, R. F., D. Zamith-Miranda, I. F. Munhoz da Rocha, A. C. R. Lucena, S. de Toledo Martins *et al.*, 2022 Caspofungin Affects Extracellular Vesicle Production and Cargo in Candida auris. J Fungi (Basel) 8.

Artuyants, A., T. L. Campos, A. K. Rai, P. J. Johnson, P. Dauros-Singorenko *et al.*, 2020 Extracellular vesicles produced by the protozoan parasite Trichomonas vaginalis contain a preferential cargo of tRNA-derived small RNAs. International Journal for Parasitology 50**:** 1145-1155.

Bielska, E., M. A. Sisquella, M. Aldeieg, C. Birch, E. J. O'Donoghue *et al.*, 2018 Pathogen-derived extracellular vesicles mediate virulence in the fatal human pathogen *Cryptococcus gattii*. Nature communications 9**:** 1556-1556.

Bitencourt, T. A., O. Hatanaka, A. M. Pessoni, M. S. Freitas, G. Trentin *et al.*, 2022a Fungal extracellular vesicles are involved in intraspecies intracellular communication. mBio 13**:** e0327221.

Bitencourt, T. A., A. M. Pessoni, B. T. M. Oliveira, L. R. Alves and F. Almeida, 2022b The RNA content of fungal extracellular vesicles: at the "cutting-edge" of pathophysiology regulation. Cells 11.

Brown, L., J. M. Wolf, R. Prados-Rosales and A. Casadevall, 2015 Through the wall: extracellular vesicles in Gram-positive bacteria, mycobacteria and fungi. Nat Rev Microbiol 13**:** 620-630.

Buck, A. H., G. Coakley, F. Simbari, H. J. McSorley, J. F. Quintana *et al.*, 2014 Exosomes secreted by nematode parasites transfer small RNAs to mammalian cells and modulate innate immunity. Nature Communications 5488**:** doi:10.1038/ncomms6488.

Cai, Q., B. He, S. Wang, S. Fletcher, D. Niu *et al.*, 2021 Message in a Bubble: Shuttling Small RNAs and Proteins Between Cells and Interacting Organisms Using Extracellular Vesicles. Annual Review of Plant Biology 72**:** 497-524.

Canzler, S., P. F. Stadler and J. Schor, 2018 The fungal snoRNAome. Rna 24**:** 342-360.

Chan, Patricia P., Brian Y. Lin, Allysia J. Mak and Todd M. Lowe, 2021 tRNAscan-SE 2.0: improved detection and functional classification of transfer RNA genes. Nucleic Acids Research 49**:** 9077-9096.

Chiou, N. T., R. Kageyama and K. M. Ansel, 2018 Selective Export into Extracellular Vesicles and Function of tRNA Fragments during T Cell Activation. Cell Rep 25**:** 3356-3370.e3354.

Chow, F. W., G. Koutsovoulos, C. Ovando-Vázquez, K. Neophytou, J. R. Bermúdez-Barrientos *et al.*, 2019 Secretion of an Argonaute protein by a parasitic nematode and the evolution of its siRNA guides. Nucleic Acids Res 47**:** 3594-3606.

Cui, C., Y. Wang, J. Liu, J. Zhao, P. Sun *et al.*, 2019 A fungal pathogen deploys a small silencing RNA that attenuates mosquito immunity and facilitates infection. Nature Communications 10**:** 4298.

D'Souza, C. A., J. W. Kronstad, G. Taylor, R. Warren, M. Yuen *et al.*, 2011 Genome variation in *Cryptococcus gattii*, an emerging pathogen of immunocompetent hosts. mBio 2**:** e00342-00310.

Dumesic, P. A., P. Natarajan, C. Chen, I. A. Drinnenberg, B. J. Schiller *et al.*, 2013 Stalled spliceosomes are a signal for RNAi-mediated genome defense. Cell 152**:** 957-968.

Edgar, R. C., 2004 MUSCLE: multiple sequence alignment with high accuracy and high throughput. Nucleic Acids Res 32**:** 1792-1797.

Fisher, M. C., and D. W. Denning, 2023 The WHO fungal priority pathogens list as a game-changer. Nat Rev Microbiol 21**:** 211-212.

Ford, T., J. Graham and D. Rickwood, 1994 Iodixanol: a nonionic iso-osmotic centrifugation medium for the formation of self-generated gradients. Anal. Biochem. 220**:** 360-366.

Gámbaro, F., M. Li Calzi, P. Fagúndez, B. Costa, G. Greif *et al.*, 2020 Stable tRNA halves can be sorted into extracellular vesicles and delivered to recipient cells in a concentration-dependent manner. RNA Biol 17**:** 1168-1182.

Gonzalez-Hilarion, S., D. Paulet, K.-T. Lee, C.-C. Hon, P. Lechat *et al.*, 2016 Intron retention-dependent gene regulation in *Cryptococcus neoformans*. Scientific Reports 6: 32252.

Gröhs Ferrareze, P. A., C. Maufrais, R. Silva Araujo Streit, S. J. Priest, C. A. Cuomo *et al.*, 2021 Application of an optimized annotation pipeline to the *Cryptococcus deuterogattii* genome reveals dynamic primary metabolic gene clusters and genomic impact of RNAi loss. G3 (Bethesda) 11.

Gruner, H. N., and M. T. McManus, 2021 Examining the evidence for extracellular RNA function in mammals. Nature Reviews Genetics 22: 448-458.

Honorato, L., J. F. D. de Araujo, C. C. Ellis, A. C. Piffer, Y. Pereira *et al.*, 2022 Extracellular vesicles regulate biofilm formation and yeast-to-hypha differentiation in *Candida albicans*. mBio 13: e0030122.

Hulstaert, E., A. Morlion, F. Avila Cobos, K. Verniers, J. Nuytens *et al.*, 2020 Charting Extracellular Transcriptomes in The Human Biofluid RNA Atlas. Cell Reports 33: 108552.

Janbon, G., S. Y. Maeng, D-F., Y.-J. Ko, K.-W. Jung, F. Moyrand *et al.*, 2010 Characterizing the role of RNA silencing components in *Cryptococcus neoformans*. Fungal Genet. Biol. 47: 1070-1080.

Janbon, G., K. L. Ormerod, D. Paulet, E. J. Byrnes III, G. Chatterjee *et al.*, 2014 Analysis of the genome and transcriptome of *Cryptococcus neoformans* var. *grubii* reveals complex RNA expression and microevolution leading to virulence attenuation. PLoS Genet. 10: e1004261.

Jöchl, C., M. Rederstorff, J. Hertel, P. F. Stadler, I. L. Hofacker *et al.*, 2008 Small ncRNA transcriptome analysis from Aspergillus fumigatus suggests a novel mechanism for regulation of protein synthesis. Nucleic Acids Res 36: 2677-2689.

Johnson, N. R., L. F. Larrondo, J. M. Álvarez and E. A. Vidal, 2022 Comprehensive re-analysis of hairpin small RNAs in fungi reveals loci with conserved links. eLife 11: e83691.

Kalem, M. C., and J. C. Panepinto, 2022 Long Non-Coding RNAs in Cryptococcus neoformans: Insights Into Fungal Pathogenesis. Front Cell Infect Microbiol 12: 858317.

Kalvari, I., E. P. Nawrocki, N. Ontiveros-Palacios, J. Argasinska, K. Lamkiewicz *et al.*, 2021 Rfam 14: expanded coverage of metagenomic, viral and microRNA families. Nucleic Acids Res 49: D192-d200.

Kim, D., G. Pertea, C. Trapnell, H. Pimentel, R. Kelley *et al.*, 2013 TopHat2: accurate alignment of transcriptomes in the presence of insertions, deletions and gene fusions. Genome biology 14: R36-R36.

Kumar, P., C. Kuscu and A. Dutta, 2016 Biogenesis and Function of Transfer RNA-Related Fragments (tRFs). Trends Biochem Sci 41: 679-689.

Kwon-Chung, K. J., J. A. Fraser, T. L. Doering, Z. Wang, G. Janbon *et al.*, 2014 *Cryptococcus neoformans* and *Cryptococcus gattii*, the etiologic agents of cryptococcosis. Cold Spring Harb Perspect Med 4: a019760.

Lambertz, U., M. E. Oviedo Ovando, E. J. R. Vasconcelos, P. J. Unrau, P. J. Myler *et al.*, 2015 Small RNAs derived from tRNAs and rRNAs are highly enriched in exosomes from both old and new world Leishmania providing evidence for conserved exosomal RNA Packaging. BMC Genomics 16: 151.

Langmead, B., and S. L. Salzberg, 2012 Fast gapped-read alignment with Bowtie 2. Nat Methods 9: 357-359.

Liu, M., Z. Zhang, C. Ding, T. Wang, B. Kelly *et al.*, 2020 Transcriptomic Analysis of Extracellular RNA Governed by the Endocytic Adaptor Protein Cin1 of Cryptococcus deneoformans. Front Cell Infect Microbiol 10: 256.

Loftus, B., E. Fung, P. Roncaglia, D. Rowley, P. Amedeo *et al.*, 2005 The genome and transcriptome of *Cryptococcus neoformans*, a basidiomycetous fungal pathogen of humans. Science 307: 1321-1324.

Ma, H., F. Hagen, D. J. Stekel, S. A. Johnston, E. Sionov *et al.*, 2009 The fatal fungal outbreak on Vancouver Island in characterized by enhanced intracellular parasitism driven by mitochondrial regulation. Proc. Natl. Acad. Sci. USA 106: 12980-12985.

Maute, R. L., C. Schneider, P. Sumazin, A. Holmes, A. Califano *et al.*, 2013 tRNA-derived microRNA modulates proliferation and the DNA damage response and is down-regulated in B cell lymphoma. Proceedings of the National Academy of Sciences 110**:** 1404-1409.

Moyrand, F., I. Lafontaine, T. Fontaine and G. Janbon, 2008 *UGE1* and *UGE2* regulate the UDP-glucose/UDP-galactose equilibrium in *Cryptococcus neoformans*. Eukaryotic Cell 7**:** 2069-2077.

Munhoz da Rocha, I. F., R. F. Amatuzzi, A. C. R. Lucena, H. Faoro and L. R. Alves, 2020 Cross-Kingdom extracellular vesicles EV-RNA communication as a mechanism for host-pathogen interaction. Front Cell Infect Microbiol 10**:** 593160.

Munhoz da Rocha, I. F., S. T. Martins, R. F. Amatuzzi, D. Zamith-Miranda, J. D. Nosanchuk *et al.*, 2021 Cellular and Extracellular Vesicle RNA Analysis in the Global Threat Fungus Candida auris. Microbiol Spectr 9**:** e0153821.

Nielsen, K., G. M. Cox, P. Wang, D. L. Toffaletti, J. R. Perfect *et al.*, 2003 Sexual cycle of *Cryptococcus neoformans* var. *grubii* and virulence of congenic **a** and alpha isolates. Infection and Immunity 71**:** 4831-4841.

Pandey, K. K., D. Madhry, Y. S. Ravi Kumar, S. Malvankar, L. Sapra *et al.*, 2021 Regulatory roles of tRNA-derived RNA fragments in human pathophysiology. Molecular Therapy - Nucleic Acids 26**:** 161-173.

Peres da Silva, R., S. d. T. Martins, J. Rizzo, F. C. G. Dos Reis, L. S. Joffe *et al.*, 2018 Golgi Reassembly and Stacking Protein (GRASP) Participates in Vesicle-Mediated RNA Export in Cryptococcus Neoformans. Genes 9**:** 400.

Peres da Silva, R., R. Puccia, M. L. Rodrigues, D. L. Oliveira, L. S. Joffe *et al.*, 2015 Extracellular vesicle-mediated export of fungal RNA. Scientific Reports 5**:** 7763.

Pita, T., J. R. Feliciano and J. H. Leitão, 2020 Extracellular RNAs in Bacterial Infections: From Emerging Key Players on Host-Pathogen Interactions to Exploitable Biomarkers and Therapeutic Targets. Int J Mol Sci 21.

Rajasingham, R., R. M. Smith, B. J. Park, J. N. Jarvis, N. P. Govender *et al.*, 2017 Global burden of disease of HIV-associated cryptococcal meningitis: an updated analysis. The Lancet Infectious Diseases 17**:** 873-881.

Reis, F. C. G., B. S. Borges, L. J. Jozefowicz, B. A. G. Sena, A. W. A. Garcia *et al.*, 2019 A novel protocol for the isolation of fungal extracellular vesicles reveals the participation of a putative scramblase in polysaccharide export and capsule construction in *Cryptococcus gattii*. mSphere 4**:** e00080-00019.

Reis, F. C. G., B. Gimenez, L. J. Jozefowicz, R. F. Castelli, S. T. Martins *et al.*, 2021 Analysis of Cryptococcal Extracellular Vesicles: Experimental Approaches for Studying Their Diversity Among Multiple Isolates, Kinetics of Production, Methods of Separation, and Detection in Cultures of Titan Cells. Microbiol Spectr 9**:** e0012521.

Ren, B., X. Wang, J. Duan and J. Ma, 2019 Rhizobial tRNA-derived small RNAs are signal molecules regulating plant nodulation. Science 365**:** 919-922.

Rice, P., I. Longden and A. Bleasby, 2000 EMBOSS: the European Molecular Biology Open Software Suite. Trends Genet 16**:** 276-277.

Rimer, J. M., J. Lee, C. L. Holley, R. J. Crowder, D. L. Chen *et al.*, 2018 Long-range function of secreted small nucleolar RNAs that direct 2'-O-methylation. Journal of Biological Chemistry 293**:** 13284-13296.

Rizzo, J., M. L. Rodrigues and G. Janbon, 2020 Extracellular vesicles in fungi: past, present and future perspectives. Frontiers in Cellular and Infection Microbiology**:** in press.

Rizzo, J., A. Taheraly and G. Janbon, 2021a Structure, composition and biological properties of fungal extracellular vesicles. microLife 2.

Rizzo, J., A. Trottier, F. Moyrand, J. Y. Coppée, C. Maufrais *et al.*, 2023 Coregulation of extracellular vesicle production and fluconazole susceptibility in Cryptococcus neoformans. mBio**:** e0087023.

Rizzo, J., S. S. W. Wong, A. D. Gazi, F. Moyrand, T. Chaze *et al.*, 2021b *Cryptococcus* extracellular vesicles properties and their use as vaccine platforms. Journal of Extracellular Vesicles 10**:** e12129.

Rodrigues, M. L., L. Nimrichter, D. L. Oliveira, S. Frases, K. Miranda *et al.*, 2007 Vesicular polysaccharide export in *Cryptococcus neoformans* is a eukaryotic solution to the problem of fungal trans-cell wall transport. Eukaryotic Cell 6**:** 48-59.

Rutter, B. D., T. T. Chu, J. F. Dallery, K. K. Zajt, R. J. O'Connell *et al.*, 2022 The development of extracellular vesicle markers for the fungal phytopathogen *Colletotrichum higginsianum*. Journal of Extracellular Vesicles 11**:** e12216.

Sahr, T., P. Escoll, C. Rusniok, S. Bui, G. Pehau-Arnaudet *et al.*, 2022 Translocated *Legionella pneumophila* small RNAs mimic eukaryotic microRNAs targeting the host immune response. Nature Communications 13**:** 762.

Schwanhäusser, B., D. Busse, N. Li, G. Dittmar, J. Schuchhardt *et al.*, 2011 Global quantification of mammalian gene expression control. Nature 473**:** 337-342.

Sharma, M., H. Zhang, G. Ehrenkaufer and U. Singh, 2023 Stress Response in Entamoeba histolytica Is Associated with Robust Processing of tRNA to tRNA Halves. mBio 14**:** e0345022.

Tsatsaronis, J. A., S. Franch-Arroyo, U. Resch and E. Charpentier, 2018 Extracellular Vesicle RNA: A Universal Mediator of Microbial Communication? Trends Microbiol. 26**:** 401-410.

Valadi, H., K. Ekström, A. Bossios, M. Sjöstrand, J. J. Lee *et al.*, 2007 Exosome-mediated transfer of mRNAs and microRNAs is a novel mechanism of genetic exchange between cells. Nature Cell Biology 9**:** 654-659.

van Niel, G., D. R. F. Carter, A. Clayton, D. W. Lambert, G. Raposo *et al.*, 2022 Challenges and directions in studying cell–cell communication by extracellular vesicles. Nat. Rev. Mol. Cell. Biol. 23**:** 369-382.

van Niel, G., G. D'Angelo and G. Raposo, 2018 Shedding light on the cell biology of extracellular vesicles. Nat. Rev. Mol. Cell. Biol. 19**:** 213-228.

Wallace, E. W. J., C. Maufrais, J. Sales-Lee, L. R. Tuck, L. de Oliveira *et al.*, 2020 Quantitative global studies reveal differential translational control by start codon context across the fungal kingdom. Nucleic Acids Research 48**:** 2312-2331.

Weaver, A. M., and J. G. Patton, 2020 Argonautes in Extracellular Vesicles: Artifact or Selected Cargo? Cancer Res 80**:** 379-381.

Weiberg, A., M. Wang, F. M. Lin, H. Zhao, Z. Zhang *et al.*, 2013 Fungal small RNAs suppress plant immunity by hijacking host RNA interference pathways. Science 342**:** 118-123.

Yadav, V., S. Sun, R. B. Billmyre, B. C. Thimmappa, T. Shea *et al.*, 2018 RNAi is a critical determinant of centromere evolution in closely related fungi. Proc Natl Acad Sci U S A 115**:** 3108-3113.

Zarnowski, R., A. Noll, M. G. Chevrette, H. Sanchez, R. Jones *et al.*, 2021 Coordination of fungal biofilm development by extracellular vesicle cargo. Nature Communications 12**:** 6235.